INTERNATIONAL JOURNAL OF HYDROGEN ENERGY 39 (2014) 7735–7746

Available online at www.sciencedirect.com

ScienceDirect

journal homepage: www.elsevier.com/locate/he

Steam reforming of ethanol over Ni-based catalysts: Effect of feed composition on catalyst stability

R. Trane-Restrup [a], S. Dahl [b], A.D. Jensen [a,*]

[a] Department of Chemical and Biochemical Engineering, Technical University of Denmark, Søltofts Plads, Building 229, 2800 Kgs. Lyngby, Denmark

[b] Department of Physics, Technical University of Denmark, Building 307, 2800 Kgs. Lyngby, Denmark

ARTICLE INFO

Article history:
Received 31 December 2013
Received in revised form
9 March 2014
Accepted 16 March 2014
Available online 14 April 2014

Keywords:
Steam reforming
Ethanol
Nickel
Carbon deposition
Oxygen addition
Hydrogen addition

ABSTRACT

In this work the effects of steam-to-carbon ratio (S/C), and addition of H_2 or O_2 to the feed on the product yields and carbon deposition in the steam reforming (SR) of ethanol over Ni/$MgAl_2O_4$, Ni/$Ce_{0.6}Zr_{0.4}O_2$, and Ni/CeO_2 at 600 °C have been investigated. Increasing the S/C-ratio from 1.6 to 8.3 over Ni/$MgAl_2O_4$ increased conversion of ethanol as well as the yield of H_2, while the carbon deposition and yield of hydrocarbons decreased. Oxygen addition at S/C-ratio of 6 over Ni/$MgAl_2O_4$, Ni/$Ce_{0.6}Zr_{0.4}O_2$, and Ni/CeO_2 increased conversion, decreased the yield of hydrocarbons, and led to a decrease in the carbon deposition. Carbon deposition was almost eliminated over Ni/$MgAl_2O_4$ and Ni/$Ce_{0.6}Zr_{0.4}O_2$ at an O/C-ratio of roughly 0.8 or higher. The penalty of adding O_2 was a decrease in the yield of H_2 from 70% at O/C = 0 to 50% at O/C = 0.8–1.

A 90 h test at O/C = 1.1, S/C = 6, and 600 °C over Ni/$MgAl_2O_4$ showed stable behavior and an average rate of carbon deposition of less than 7 μg C/g_{Cat} h. The results indicate that stable operation of ethanol SR is only possible under oxidative conditions.

Introduction

Biomass is the only sustainable carbon source available and liquid fuels, like diesel and gasoline, might be produced from biomass in the future. However, biomass has a low energy density and is therefore expensive to transport over longer distances [1]. One possibility is to do a flash pyrolysis of the biomass, which, among other products, yields a liquid fraction called bio-oil or pyrolysis oil. The flash pyrolysis can be tuned to obtain a maximum yield of bio-oil around 75 wt% from wood and barley straw [2–5]. The advantage of converting biomass into bio-oil is lower transportation costs due to an up to ten times higher energy density of bio-oil compared with untreated biomass [1–4].

Abbreviations: HDO, hydrodeoxygenation; MAR, mass action ratio; SR, steam reforming; WGS, water gas shift; WHSV, weight hourly space velocity.

* *Corresponding author.* Tel.: +45 4525 2841; fax: +45 4588 2258.
E-mail address: aj@kt.dtu.dk (A.D. Jensen).

http://dx.doi.org/10.1016/j.ijhydene.2014.03.107
0360-3199/

Bio-oil contains mainly oxygenated compounds, which nevertheless induces a low heating value compared to fossil fuels as well as a low storage stability [6]. Polymerization of oxygenates in the bio-oil upon storage may increase the viscosity and lead to phase separation [6–8]. These issues make the bio-oil unsuited for direct utilization as a fuel and therefore upgrading of the bio-oil is needed. Thus, one concept for bio-oil utilization could be to conduct the flash pyrolysis of biomass close to the biomass production site and then transport the bio-oil to a (bio)refinery. Here upgrading of the oil through prospective catalytic processes like hydrodeoxygenation (HDO) or steam reforming (SR) can be performed [9–11]. HDO needs hydrogen to upgrade the bio-oil to transportation fuels, which can be produced through SR of bio-oil making the overall process sustainable [9,12–14]. One of the main challenges in SR of bio-oil is deactivation of catalysts due to carbon deposition on the catalysts [9,13–17], which will be addressed in this study.

In this study ethanol has been chosen as a model compound of bio-oil because it has an oxygen functionality which is found in bio-oil and similar to bio-oil is prone to carbon deposition on the catalysts leading to deactivation [18–20]. Furthermore SR of ethanol is in its own an interesting process as it can be used to provide for H_2 for fuel cells in mobile applications [21].

Steam reforming of ethanol can be described by the following reactions:

$$CH_3CH_2OH + H_2O \rightleftharpoons 2CO + 4H_2 \quad (1)$$

$$CH_3CH_2OH + 3H_2O \rightleftharpoons 2CO_2 + 6H_2 \quad (2)$$

Reaction (1) is the general SR-reaction, while Reaction (2) assumes full shift of CO to CO_2 (Reaction (3)), which yields two additional moles of H_2. Beside the water-gas shift (WGS) reaction, the methanation reaction may also influence the product distribution:

$$CO + H_2O \rightleftharpoons CO_2 + H_2 \quad (3)$$

$$CO + 3H_2 \rightleftharpoons CH_4 + H_2O \quad (4)$$

The offgas composition is governed by the kinetics and equilibrium between the reactions shown above e.g. Reactions (1), (3), and (4). High temperatures will favor the reforming reaction and produce H_2 and CO as Reaction (1) is shifted toward the right, while Reaction (4) will be shifted to the left. The WGS, Reaction (3), will be shifted toward CO and H_2O at temperatures above 800 °C and therefore the maximum H_2 production is achieved at intermediate temperatures, 600–800 °C [22].

Side reactions observed in SR of ethanol are dehydration, Reaction (5), or dehydrogenation, Reaction (6), yielding ethene and acetaldehyde, respectively [21,23–28].

$$CH_3CH_2OH \rightarrow C_2H_4 + H_2O \quad (5)$$

$$CH_3CH_2OH \rightarrow C_2H_4O + H_2 \quad (6)$$

Especially, formation of ethene is troublesome as it has a high potential for forming carbon deposits [26,29–31]. Carbon formation from ethene could occur through decomposition followed by accumulation and polymerization of carbon atoms [25,29,31]:

$$C_2H_4 \rightarrow 2C + 2H_2 \rightarrow Carbon \quad (7)$$

Alternatively, carbon deposits can be formed through direct polymerization of ethene [21,23,24]:

$$nC_2H_4 \rightarrow Carbon \quad (8)$$

Others routes to carbon deposition includes the Boudouard reaction (Reaction (9)), CO decomposition (Reaction (10)), and methane decomposition (Reaction (11)).

$$2CO \rightleftharpoons C_s + CO_2 \quad (9)$$

$$CO + H_2 \rightleftharpoons C_s + H_2O \quad (10)$$

$$CH_4 \rightleftharpoons C_s + 2H_2 \quad (11)$$

The carbon formed in Reactions (7)–(11), can be as carbon whiskers or gum depending on the temperature [32–34]. Carbon deposition is discussed further in the Supplementary Data.

Oxidative SR can be used to decrease carbon deposition as oxygen may react with carbon or carbon precursors on the surface of the catalysts. However, oxidative conditions will increase the formation of CO_2 and decrease H_2-production [13,35–44]. Among others, Cavallaro et al. [18] reported a decrease in carbon deposition from 0.28 mg/(g_{Cat} h) to 0.01 mg/(g_{Cat} h) at 650 °C and S/C-ratio of 4.2 over Rh/Al_2O_3 when adding O_2 to the feed gas at an O/C-ratio of 0.4. No carbon was deposited on a $La_{0.9}Ce_{0.1}NiO_3$-perovskite catalyst operated at 300–800 °C, S/C = 1.5, and O/C = 0.5 [41]. Furthermore it was shown that O/C-levels lower than 0.5 led to carbon deposition over $La_{0.9}Ce_{0.1}NiO_3$ at S/C = 1.5 and 500 °C [41]. The yield of H_2 depends on both S/C-ratio and O/C-ratio and Salge et al. [42] reported a maximum yield of H_2 in SR of ethanol under oxidative conditions of 57.5%, according to the definition of yield used in this work, at 600 °C, S/C = 4.5, and O/C = 0.66 over a Rh–Ce monolith catalyst. Peela and Kunzru [43] reported a drop in the yield of H_2 at 550 °C and S/C = 3 from 65% at O/C = 0 to 43% at O/C = 1.5. These results indicate that addition of oxygen to the feed may help solve the carbon deposition problem, but at the cost of a lower yield of H_2.

Another strategy to minimize the carbon deposition problem would be to add hydrogen to the feed. Hydrogen might hydrogenate unsaturated compounds like ethene and therefore decrease the deposition of carbon. Furthermore the additional H_2 will ensure that the catalyst is reduced under the reaction conditions. Laosiripojana et al. [44] investigated addition of H_2 at H/C-ratios between 0 and 5 at S/C-ratio of 1.5 and found a decrease in hydrocarbon yield and carbon deposition on Ni/CeO_2 and Ni/Al_2O_3 at 900 °C in SR of ethanol. The yield of CH_4 decreased from 10.6% at H/C = 0–7.1% at H/C = 5, while the carbon deposition decreased from 1.08 monolayers at H/C = 0–0.13 monolayers at H/C = 5 over Ni/CeO_2. Jacobs et al. [45] reported an increased conversion and methane formation with hydrogen addition over Pt/CeO_2 at 300 °C, S/C-ratio of 16.7, and H/C-ratios between 0 and 26.7 in the SR of acetic acid. The conversion increased from 5.4% at H/C = 0 to 35.6% at H/C = 26.7, while the yield of CH_4 increased

from 28% at H/C = 0 to 49.4% at H/C = 26.7. The opposite effect of H_2 on the methane formation between Laosiripojana et al. [44] and Jacobs et al. [45] might be ascribed to the effect of temperature on the equilibrium. At temperatures below 500 °C methanation of CO and CO_2 is thermodynamically favorable while at temperatures above 500 °C the equilibrium will be shifted toward carbon oxides. Therefore the effect of H_2 might be an increased rate of reaction, which brings the product gas closer to equilibrium i.e. methane at temperatures below 500 °C and carbon oxides above 600 °C.

There is a lack of quantitative studies of the effects of the feed composition in terms of both H_2O, O_2, and H_2 concentrations on carbon deposition and gas product yields during SR of ethanol. In this work, the addition of H_2, O_2, and H_2O to the feed gas in SR of ethanol has been tested systematically to elucidate the effects on carbon deposition, conversion, and product yields.

Experimental

Catalyst preparation

Several catalysts were prepared by incipient wetness impregnation with a $Ni(NO_3)_2$-solution on three different carriers as explained in detail in ref. 46; CeO_2 (AMR Ltd., 141 m^2/g), $Ce_{0.6}Zr_{0.4}O_2$ (AMR Ltd., 137 m^2/g), and $MgAl_2O_4$ (Puralox MG30/150 from Sasol, 150 m^2/g). $Ni(NO_3)_2 \cdot 6H_2O$ (Sigma–Aldrich, >97% pure) was dissolved in a volume of water corresponding to the pore volume of the dry carrier. The solution was mixed with the dry carrier material and stirred. The wet powder was dried at 110 °C overnight in air and calcined at 800 °C (heating rate 10 °C/min) for 2 h in stagnant air.

Experimental setup

The flowsheet of the experimental setup used in this study is shown in Fig. S1 in the Supplementary Data. Briefly, the setup consisted of a gas supply section where up to eight different gases could be connected, a liquid reactant supply section where two bubble columns were used to supply water and ethanol. In each bubble column, N_2 flows were saturated with ethanol or water at 60 °C and 79 °C, respectively, and led to the reactor. The feed evaporation system was tested prior to the experiments and worked at 80% and 90% efficiency for ethanol and water, respectively. The gases were transported in lines heated to 110 °C to a quartz reactor placed in a three zone furnace. The effluent from the reactor passed through a condenser operated at 6–7 °C, which collected liquid products, H_2O, and unconverted ethanol. After the condenser the gases passed the analysis section, which consisted of a Varian MicroGC CP-4900 and a 5-channel Rosemount NGA 2000 on-line gas analyzer. The MicroGC had two columns, a molecular sieve 5A and a PoraPlot Q, and two thermal conductivity detectors (TCD), which measured the concentrations of CO, CO_2, H_2, CH_4, C_2H_4, and C_2H_6. GC measurements were conducted every 10 min and representative measurements for every 30–60 min is used to show transient behavior. The on-line gas analyzer uses IR to measure the CO, CO_2, and O_2 concentrations continuously and data points were collected every 30–60 s.

Table 1 – General reaction conditions. N_2 as balance gas in all experiments.

Flow [N mL/min]	Ethanol [vol%]	H_2O [vol%]	O_2 [vol%]	H_2 [vol%]
1500–1600	3.0–3.5	10–50	0–6.3	0–3.6

The catalyst was placed between two pieces of quartz wool resting on a quartz frit inside a quartz tube with an inner diameter of 17 mm. The steam and ethanol were fed from the top of the reactor through an inlet tube with an inner diameter of 4 mm and perforated with 12 holes in the end to disperse the gas over catalyst bed. The outlet of the inlet/feeding tube was approx. 5 cm above the catalyst bed allowing time for mixing the two gas streams while minimizing homogeneous gas phase reactions before reaching the catalyst. The temperature was measured by a thermocouple just below the quartz frit.

Long term experiments (≥24 h) were conducted with a different feeding system for ethanol and water in order to obtain stable flows. Here the desired mixture of water and ethanol was pumped through an evaporator operated at 250 °C and then fed to the reactor through the feeding tube along with N_2 for dilution. The pump was a Knauer Smartline 100 pump and the evaporator consisted of a stainless steel tube with an outer diameter of 3.175 mm wrapped around a copper core heated by a heating cartridge. Similar results were obtained with the two feeding systems, see Tables S1 and S2 in the Supplementary Data.

Catalytic test

0.5 g of catalyst with a particle size of 250–425 μm was loaded into the reactor, resulting in a bed with a height of roughly 3–4 mm in height which means that the flow in the bed was in between plug flow and mixed flow [47]. In principle mixed flow would have been desirable since all catalyst pellets would then be exposed to identical conditions. The catalyst was first heated to 600 °C in a flow of N_2 and at 600 °C the flow was changed to a 50/50 flow of N_2 and H_2 of roughly 500 N mL/min for 1 h. After reduction, the reactor was purged with N_2 for 10 min and then the reactants were directed to the reactor. The general conditions of the experiments can be seen in Table 1. The lower flammability limits of ethanol in air is 4 vol % [48], so the mixture should not be able to ignite under the reaction conditions.

Diffusion limitations were estimated by Weisz-Prater and Mears criteria. The value of Weisz-Prater criteria for the largest particle size, 425 μm, was 0.45, while Mears criteria was 0.01 for the same particle size indicating that diffusion limitations did not exist at the applied experimental conditions.

Determination of the amount of carbon deposited

The amount of carbon deposited during an experiment was determined by temperature programmed oxidation (TPO), where the spent catalysts were heated from 200 to 700 °C (10 °C/min) in a flow of 1000 NmL/min of 2–3% O_2 in N_2. The evolution of CO and CO_2 was monitored by the online gas analyzer (sampling rate: 0.2 s^{-1}) and the amount of carbon on the catalyst was determined by integration of these signals.

Catalyst characterization

The BET surface area of the prepared catalysts was measured by N_2 adsorption at its boiling point using multipoint BET theory with seven points in the $p/p_0 = 0.05–0.3$ range using a Quantachrome iQ2.

XRD patterns were recorded for fresh catalysts, prior to reduction, and the spent catalysts, after TPO, by a PANalytical X'Pert PRO Diffractometer, which had a rotating sample holder, a rotating copper anode X-ray source, nickel filter, and automatic anti-scatter and divergence slits. Particle sizes of NiO were determined by the line broadening of the peaks in the XRD patterns through the Scherrer equation [49]:

$$d_p = \frac{K \cdot \lambda}{\beta \cdot \cos(\theta)} \tag{12}$$

where K is a shape factor set to 0.9 [49], λ is the X-ray wavelength, β is the full width at half maximum corrected for the instrumental line broadening, while θ is the Bragg angle. The size of the NiO particles is used as measure of Ni particle size and to evaluate the change in particle size during an experiment. Reduction without sintering of the Ni-particles would lead to Ni-particles, which are 16% smaller than the NiO particles.

Calculations

The S/C, O/C, and H/C-ratio are defined as:

$$S/C = \frac{n_{H_2O,\,in}}{2 \cdot n_{Eth,\,in}} \tag{13}$$

$$O/C = \frac{n_{O_2,\,in}}{n_{Eth,\,in}} \tag{14}$$

$$H/C = \frac{n_{H_2,\,in}}{n_{Eth,\,in}} \tag{15}$$

The weight hourly space velocity, $WHSV$, is defined as mass flow of ethanol pr. mass of catalyst:

$$WHSV = \frac{F_{m,\,Eth}}{m_{Cat}} \; [h^{-1}] \tag{16}$$

The conversion of ethanol is calculated on a carbon basis as:

$$X = \frac{\sum n_{C,\,i} \cdot n_i}{2 \cdot n_{Eth,\,in}} \cdot 100\% \; [\%] \tag{17}$$

where n_i is the number of moles of compound i produced and $n_{C,i}$ is the number of carbon atoms in that compound.

The yield of products are calculated using the definition in Fogler [50]:

$$Y_i = \frac{n_{C,\,i} \cdot n_i}{\sum n_{C,\,i} \cdot n_i} \cdot 100\% \; [\%] \tag{18}$$

The yield of H_2 is defined as:

$$Y_{H_2} = \frac{n_{H_2} - n_{H_2,\,in}}{6 \cdot n_{C_2H_6O,\,in} \cdot X} \cdot 100\% \; [\%] \tag{19}$$

The factor of 6 is the maximum moles of H_2, which can be produced through SR of one mole of ethanol assuming full shift of CO to CO_2 (Reaction (2)).

Table 2 – Nominal metal loading, surface area, and NiO particle size of the fresh catalysts prior to reduction. XRD reflection peak from NiO at $2\theta = 62.8°$ used for determination of particle size.

Catalyst	Metal loading [wt%]	Surface area [m^2/g]	NiO particle size [nm]
$Ni/Ce_{0.6}Zr_{0.4}O_2$	8.2	90	28
Ni/CeO_2	8.2	113	10
$Ni/MgAl_2O_4$	8.2	98	4

Carbon deposition is reported as the amount of carbon deposited pr. carbon fed to the reactor, mole C/mole C_{Feed}, and in mass of carbon formed pr. mass of catalyst and time, mg C/g_{Cat} h.

Results and discussion

$Ni/MgAl_2O_4$ has been used as catalyst in most of the experimental work. However, oxidative SR over $Ni/Ce_{0.6}Zr_{0.4}O_2$ and Ni/CeO_2 catalysts are investigated to find out to what extent the effects seen in the oxidative SR over $Ni/MgAl_2O_4$ can be transferred to other catalytic systems. $Ni/MgAl_2O_4$ was chosen as the main catalyst, because it is a thermally very stable catalyst, which has proven effective in SR of hydrocarbons. It is often the choice for industrial SR units due to a good compromise between price and activity [32,33]. $Ni/MgAl_2O_4$ can be improved by addition of K and/or CeO_2, which increases conversion and decreases carbon deposition [46]. However, the promoters did not eliminate carbon deposition, and therefore it was chosen to investigate if carbon deposition over the simplest catalyst, $Ni/MgAl_2O_4$, could be eliminated by changing the feed composition.

Characterization of catalysts

The surface area, nominal metal loading, and NiO particle size for the investigated catalysts are shown in Table 2. The three support materials, CeO_2, $Ce_{0.6}Zr_{0.4}O_2$, and $MgAl_2O_4$, all yielded catalysts with surface areas in the range of 90–113 m^2/g, while the NiO particles were between 4 and 28 nm in diameter. The particle size of NiO on $MgAl_2O_4$ of 4 nm is close to the detection limit of XRD and could be uncertain. The quite large difference in particle size might influence catalyst performance as well as carbon deposition [41,51]. Generally, smaller particles increase activity and decrease carbon deposition. The XRD patterns for the three catalysts in Table 2 can be seen in Figs. S2–S4 in the Supplementary Data and confirmed that the structure of both of the mixed oxides were $Ce_{0.6}Zr_{0.4}O_2$ and $MgAl_2O_4$, respectively.

Effect of S/C-ratio

In our previous work we investigated the effect of temperature and space velocity (W/F) on the SR of ethanol over different Ni-based catalysts [46]. Based on these results the temperature 600 °C was chosen to investigate the effect of H_2, O_2, H_2O. The conversion was around 75% at this temperature, a S/C-ratio of 6, and the applied space velocity, which allows evaluation of

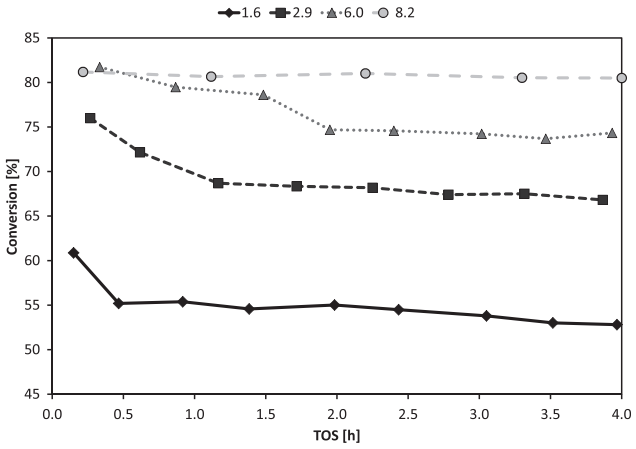

Fig. 1 – Conversion as function of time over Ni/$MgAl_2O_4$ during SR of ethanol at different S/C-ratios. Experimental conditions: Temp.: 585–590 °C; m_{Cat} = 0.50 g, Ni loading: 8.2 wt%, F_T = 1600 N mL/min, y_{Eth} = 3.0–3.3 vol%, y_{H_2O} = 10.2–50.4 vol%, N_2 as balance.

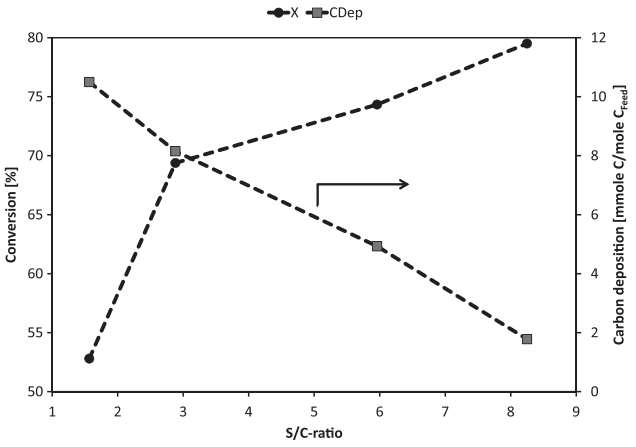

Fig. 2 – Conversion and carbon deposition after 4 h on stream as function of S/C-ratio over Ni/$MgAl_2O_4$. Experimental conditions: Temp.: 585–590 °C; m_{Cat} = 0.50 g, Ni loading: 8.2 wt%, F_T = 1600 N mL/min, y_{Eth} = 3.0–3.3 vol %, y_{H_2O} = 10.2–50.4 vol%, N_2 as balance.

changes in activity and product distribution with time on stream. In addition the propensity to carbon deposition of the reaction mixture is more clearly revealed when the conversion is kept well below 1. The products obtained in SR of ethanol over Ni-based catalysts were CO, CO_2, CH_4, C_2H_4 as well as acetone, acetic acid and acetaldehyde. The three latter compounds were only formed in trace amounts at 600 °C with a combined yield of less than 0.1%.

The S/C-ratio is important in SR as it can influence product distribution, conversion, and deactivation. The conversion as function of time at 600 °C over Ni/$MgAl_2O_4$ at four different S/C-ratios ranging from 1.6 to 8.2 is shown in Fig. 1. Deactivation was apparent in all the cases and was most pronounced at the lowest S/C-ratios. A decrease in conversion of 4–5 %-point over 4 h operation was observed for S/C-ratios between 1.6 and 6.0. At an S/C-ratio of 8.2 the decrease in conversion was significantly smaller, roughly 1%-point.

The conversion and carbon deposition after 4 h on stream as function of S/C-ratio is shown in Fig. 2. The conversion increased from 53% to 80% when the S/C-ratio increased from 1.6 to 8.2. The effect of increasing the S/C-ratio was most pronounced at low values, where an increase in conversion from 53% to 69% was observed when increasing S/C-ratio from 1.6 to 2.9. The carbon deposition decreased almost linearly with increasing S/C-ratio from 10.5 mmole C/mole C_{Feed} or 70 mg C/g_{Cat} h at S/C = 1.6 to 1.8 mmole C/mole C_{Feed} or 11 mg C/g_{Cat} h at S/C = 8.2. Both of these trends could be due to increased rate of steam gasification/reforming due to an increased amount of OH- or O-species on the catalyst from dissociative adsorption of steam.

The almost linearly decreasing carbon deposition suggests that further increments of the S/C-ratio could decrease the carbon deposition to even lower levels.

The yield of hydrogen, methane, and ethene as function of S/C-ratio can be seen in Fig. 3. The yield of hydrogen increased with S/C-ratio from 45% at S/C = 1.6 to 76% at S/C = 8.2. The approach to equilibrium for the yield of hydrogen and the CO_2/CO-ratio at different S/C-ratios can be seen in Table 3. The approach to equilibrium became closer with increasing S/C-ratio and the yield of H_2 in % of equilibrium increased from 64 to 90% when increasing the S/C-ratio from 1.6 to 8.2. Increasing the amount of steam was expected to increase the yield of hydrogen as the WGS will shift toward CO_2 and H_2. This was also seen on the CO_2/CO-ratio, which increased from about 1 at S/C = 1.6 to 4.7 at S/C = 8.2. The mass action ratio (MAR) for the WGS and methanation reactions as functions of S/C-ratio can be seen in Fig. S5 in the Supplementary Data. The MAR for WGS increased with increasing S/C-ratio showing that the product gas approached equilibrium for WGS with increasing S/C-ratio. Similar trends were observed in Refs. [18,44,52,53].

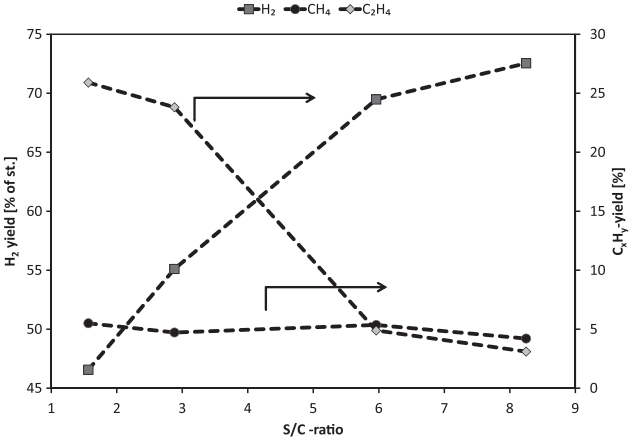

Fig. 3 – Yield of hydrogen and hydrocarbons as function of S/C-ratio over Ni/$MgAl_2O_4$ over a 4 h experiment. Experimental conditions: Temp.: 585–590 °C; m_{Cat} = 0.50 g, Ni loading: 8.2 wt%, F_T = 1600 N mL/min, y_{Eth} = 3.0–3.3 vol %, y_{H_2O} = 10.2–50.4 vol%, N_2 as balance.

Table 3 – The yield of hydrogen, equilibrium yield of hydrogen, and CO_2/CO-ratio at different S/C-ratios. Experimental conditions: Temp.: 585–590 °C; m_{Cat} = 0.50 g, Ni loading: 8.2 wt%, F_T = 1600 N mL/min, y_{Eth} = 3.0–3.3 vol%, y_{H_2O} = 10.2–50.4 vol%, N_2 as balance. eq. = equilibrium.

S/C-ratio [mole/mole]	Y_{H_2} [%]	$Y_{H_2, eq}$ [%]	CO_2/CO-ratio [mole/mole]
1.6	47	67	1
2.9	55	77	1.8
6	69	83	3.7
8.2	72	85	4.7

The yield of ethene was 26% at S/C = 1.6 and decreased to 3.1% at S/C = 8.2 and combined with the increase in conversion with S/C-ratio this could indicate that the first step in SR of ethanol over $Ni/MgAl_2O_4$ is dehydration. This indicates that the effect of increasing the S/C-ratio was to increase the overall rate of reaction, which increases the total conversion and decreases the yield of intermediates. The decrease in carbon deposition correlated well with the ethene level in the offgas (see Figs. 2 and 3) and therefore a contributing factor to the decrease in carbon deposition could be a faster SR of ethene, converting it before it is turned into solid carbon. Thermodynamical equilibrium calculations for the dehydration of ethanol show that it should be shifted toward ethene and water regardless of the water content at 600 °C. This indicates that the formation of ethene should not be limited by the higher water concentration at increasing S/C-ratios. Therefore the lower ethene concentration is likely due to faster conversion.

The yield of methane was constant at S/C-ratios from 1.6 to 8.2, indicating little influence of the steam concentration on the production and conversion of methane under SR of ethanol. The MAR for methanation (see Fig. S5) varied slightly with S/C-ratio and only a very small decrease in the MAR was observed. This again shows that the S/C-ratio has little influence on the methanation equilibrium in the SR of ethanol at the applied reaction temperature of 600 °C.

Similar to these results, a decrease in the yield of hydrocarbons with increasing S/C-ratio was also observed by Laosiripojana N, et al. [44,52].

The principle of equilibrated and actual gas was used to estimate the potential of carbon formation from methane decomposition, the Boudouard reaction, and CO decomposition [32]. There was no potential for forming carbon from an equilibrated gas, but for the actual product gas carbon deposits could form from methane decomposition at an S/C-ratio of 1.6. This shows that carbon formation is mainly from ethene, although there might be positions in the catalyst bed with a gas composition, which could have the potential to form carbon deposits through methane decomposition.

Overall, the results show that increasing the S/C-ratio increased the conversion of ethanol and yield of hydrogen while decreasing the yield of hydrocarbons and carbon deposition. Operation at high S/C-ratios seems beneficial from a stability point-of-view, but it might be uneconomical in industrial units due to a high cost for superheating the steam. Furthermore it would lead to a larger reactor, pipelines, and general equipment as the gas flow rate would be high.

Table 4 – Comparison of conversion, carbon deposition, and yield of H_2 at SR and OSR conditions after 4 h on stream over $Ni/Ce_{0.6}Zr_{0.4}O_2$, $Ni/MgAl_2O_4$, and Ni/CeO_2. Experimental conditions: S/C: 5.8–6.0; O/C: 0.19–0.28; Temp.: 579–592 °C; m_{Cat} = 0.50 g, Ni loading: 8.2 wt%, F_T = 1500 N mL/min, y_{Eth} = 3.2–3.5 vol%, y_{H_2O} = 38.4–38.6 vol%, y_{O_2} = 0.6–1.0 vol%, N_2 as balance.

Catalyst	O/C	S/C	Conversion [%]	Carbon deposition		Y_{H_2} [%]
				[mmole C/mole C_{Feed}]	[mg C/ g_{Cat} h]	
$Ni/Ce_{0.6}Zr_{0.4}O_2$	–	6.0	84	8.6	54.9	75
$Ni/Ce_{0.6}Zr_{0.4}O_2$	0.19	5.8	87	1.4	9.3	65
$Ni/MgAl_2O_4$	–	6.2	73	4.4	28.0	70
$Ni/MgAl_2O_4$	0.25	6.0	95	1.7	11.0	67
Ni/CeO_2	–	5.8	67	2.7	18.8	68
Ni/CeO_2	0.28	5.9	99	1.6	10.7	66

Oxidative steam reforming

An alternative to increasing the S/C-ratio is to co-feed oxygen, so called oxidative SR (OSR) in order to minimize the carbon deposition during SR of ethanol. The O_2 might influence the homogeneous reactions and therefore the effect of O_2 was investigated at 600 °C, S/C = 6, O/C = 0.26, and y_{O_2} = 0.8 vol% in an empty reactor. The results can be seen in Table S3 in Supplementary Data. Without O_2, equal amounts of CO, CH_4, and C_2H_4 were produced at 600 °C and the conversion of ethanol was 3%. Therefore the most important homogenous reactions were dehydration, Reaction (5), and decomposition of ethanol:

$$CH_3CH_2OH \rightarrow CH_4 + CO + H_2 \quad (20)$$

With O_2 present the product distribution was similar but the conversion was 15%. This indicates that the presence of O_2 increased the rate of homogenous dehydration and decomposition of ethanol.

The conversion of O_2 was 81% in the blank experiment with O_2 in the feed, which indicated that O_2 would reach and react on the catalysts as no O_2 was detected in the product gas in OSR experiments regardless of the inlet concentration of O_2. The conversion of O_2 was 100% in all the catalytic tests.

Oxygen co-feeding at an O/C ratio of 0.2–0.3 was tested over three different catalysts; $Ni/Ce_{0.6}Zr_{0.4}O_2$, $Ni/MgAl_2O_4$, and Ni/CeO_2. The O/C-ratios in these experiments were below what is needed for autothermal conditions which would require an O/C-ratio about 0.36 or above. Autothermal conditions are obtained when the energy from oxidation of part of the ethanol equals the energy required for SR of the remaining part of the ethanol. The calculations are based on the assumption that all the energy from combustion is used for steam reforming, not heating of gas to 600 °C.

A comparison of conversion, carbon deposition, and yield of H_2 after 4 h on stream for $Ni/Ce_{0.6}Zr_{0.4}O_2$, $Ni/MgAl_2O_4$, and Ni/CeO_2 at SR and OSR conditions can be seen in Table 4. The conversion increased for all the catalysts when adding O_2 to the feed and full conversion was achieved over Ni/CeO_2. The increase in conversion could partly be due to an increased in the rate of homogeneous reactions as an increased conversion

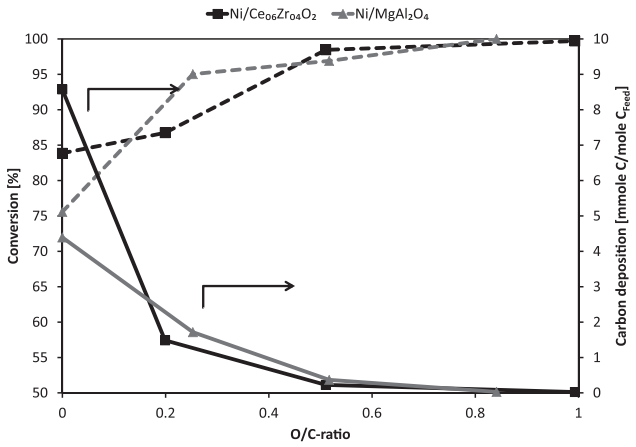

Fig. 4 – Conversion and carbon deposition after 4 h on stream as function of O/C-ratio over $Ni/MgAl_2O_4$ and $Ni/Ce_{0.6}Zr_{0.4}O_2$. Full lines are carbon deposition and dashed lines are conversion. Experimental conditions: S/C: 5.5–6.0; Temp.: 586–615 °C; m_{Cat} = 0.50 g, Ni loading: 8.2 wt%, F_T = 1600 N mL/min, y_{Eth} = 3.1–3.3 vol%, y_{H_2O} = 36.3 – 37.2 vol%, y_{O_2} = 0 – 3.2 vol%, N_2 as balance.

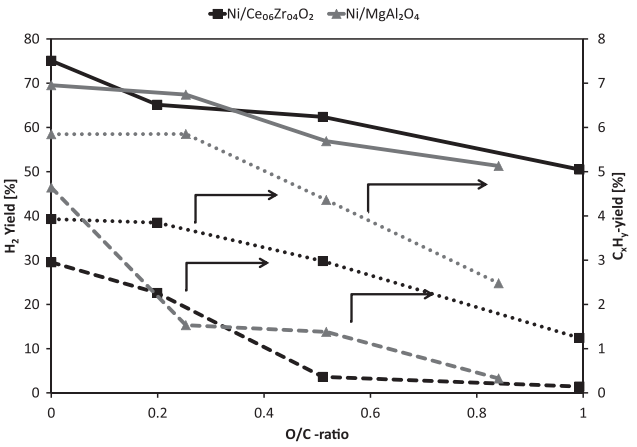

Fig. 5 – Yield of H_2, CH_4, and C_2H_4 as function of O/C-ratio over $Ni/MgAl_2O_4$ and $Ni/Ce_{0.6}Zr_{0.4}O_2$. Full lines are H_2 yield, dashed lines are C_2H_4 yield, and dotted lines are CH_4 yield. Experimental conditions: S/C: 5.5–6.0; Temp.: 586–615 °C; m_{Cat} = 0.50 g, Ni loading: 8.2 wt%, F_T = 1600 N mL/min, y_{Eth} = 3.1–3.3 vol%, y_{H_2O} = 36.3 – 37.2 vol%, y_{O_2} = 0 – 3.2 vol%, N_2 as balance.

was observed with O_2 present in an empty reactor. More importantly, O_2 facilitates surface reactions and increase conversion hereby. The carbon deposition was lower at OSR conditions for all the catalysts indicating that the O_2 present under OSR will react with carbon on the catalyst and hereby remove it and/or limit its formation by oxidizing precursor species.

In Table 4 it can also be seen that the yield of H_2 decreased at OSR-conditions with 3–12%-point, which is due to formation of CO_2 and H_2O instead of H_2 and CO.

The effect of the O/C-ratio on conversion, carbon deposition, and product distribution was investigated over $Ni/MgAl_2O_4$ and $Ni/Ce_{0.6}Zr_{0.4}O_2$. The conversion and carbon deposition after 4 h on stream as function of O/C-ratio over these catalysts are shown in Fig. 4. For $Ni/Ce_{0.6}Zr_{0.4}O_2$ the conversion increased with increasing O/C-ratio and reached nearly full conversion at an O/C-ratio of 0.5. A similar trend was observed with $Ni/MgAl_2O_4$, however the conversion increased more rapidly with addition of low amounts of oxygen and reached full conversion at an O/C-ratio of 0.84.

The carbon deposition on $Ni/Ce_{0.6}Zr_{0.4}O_2$ decreased significantly with increasing O/C-ratio and at an O/C-ratio of 0.5 only 0.2 mmole C/mole C_{Feed} or 1.5 mg C/g_{Cat} h ended up on the catalyst. Increasing the O/C-ratio to 1 decreased the carbon deposition further by approximately a factor of 10 to 0.02 mmole C/mole C_{Feed} or 0.16 mg C/g_{Cat} h. A large decrease in carbon deposition with increasing O/C-ratio was also observed over $Ni/MgAl_2O_4$. The carbon deposition at an O/C-ratio of 0.84 was 0.03 mmole C/mole C_{Feed} or 0.20 mg C/g_{Cat} h, which was similar to the results from OSR over $Ni/Ce_{0.6}Zr_{0.4}O_2$ at a similar O/C-ratio. The results indicate that O/C-ratios of roughly 1 are needed for almost carbon free operation at 600 °C over both $Ni/Ce_{0.6}Zr_{0.4}O_2$ and $Ni/MgAl_2O_4$.

When adding oxygen to the system the overall reaction changed from being endothermic at an O/C-ratio below 0.36 to exothermic at O/C-ratios above this value. This was also observed during the experiments as the reactor was almost isothermal at an O/C-ratio of 0.5, while the temperature decreased by 10 °C or increased by 10–15 °C over the catalyst bed at O/C-ratios of 0.2 and 1.0, respectively.

The yield of H_2, CH_4, and C_2H_4 as functions of the O/C-ratio over $Ni/Ce_{0.6}Zr_{0.4}O_2$ and $Ni/MgAl_2O_4$ can be seen in Fig. 5. The yield of H_2 dropped from 77% to 50% for $Ni/Ce_{0.6}Zr_{0.4}O_2$ and from 70% to 51% for $Ni/MgAl_2O_4$ when increasing the O/C-ratio from 0 to 1. This corresponds to one less mole of H_2 produced pr. mole of ethanol converted compared to SR at S/C = 6 and O/C = 0. A low temperature WGS catalyst downstream the reactor might recover part of the hydrogen as CO and steam is present in the off gas. Furthermore additional H_2 can be obtained by converting the remaining hydrocarbons to carbon oxides.

The yield of hydrocarbons over both catalysts decreased with increasing O/C-ratio. The yield of C_2H_4 decreased from 3 to 5% at O/C = 0 to zero at O/C-ratios above 0.8 for both catalysts indicating a higher rate of conversion of ethene with increasing concentration of O_2. Similarly the methane yield decreased from 5% at O/C = 0 to 1–2% at O/C-ratios above 0.8. The results show that oxidative SR is an efficient way of limiting carbon deposition but at a cost of decreasing the yield of H_2.

The MAR for WGS and methanation as function of O/C-ratio over $Ni/MgAl_2O_4$ and $Ni/Ce_{0.6}Zr_{0.4}O_2$ can be seen in Fig. S6 in the Supplementary Data. The MAR for WGS decreased slightly with increasing O/C-ratio, while the MAR for methanation increased with increasing O/C-ratio over both catalysts. This shows that oxygen is capable of converting methane under the applied conditions.

Carbon deposition in OSR is, like in SR, mainly from ethene as the principle of equilibrated and actual gas do not predict carbon formation through methane decomposition, the Boudouard reaction, or CO decomposition.

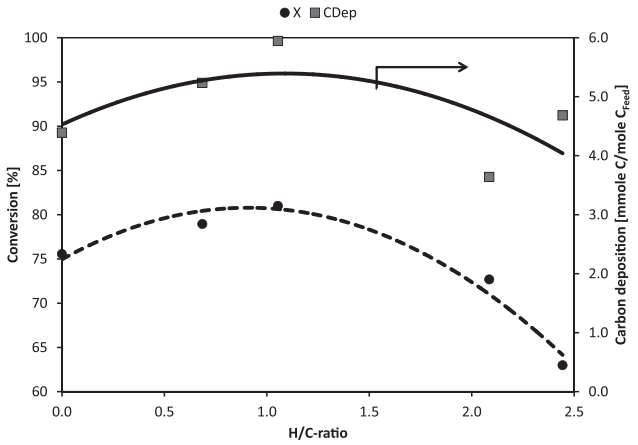

Fig. 6 – Conversion and carbon deposition after 4 h on stream as function of H/C-ratio over Ni/$MgAl_2O_4$. Full lines are carbon deposition and dashed lines are conversion. Experimental conditions: S/C: 5.9–6.0; Temp.: 586–592 °C; m_{Cat} = 0.50 g, Ni loading: 8.2 wt%, F_T = 1600 N mL/min, y_{Eth} = 3.0–3.3 vol%, y_{H_2O} = 36.0–37.2 vol%, y_{H_2} = 0–7.4 vol%, N_2 as balance.

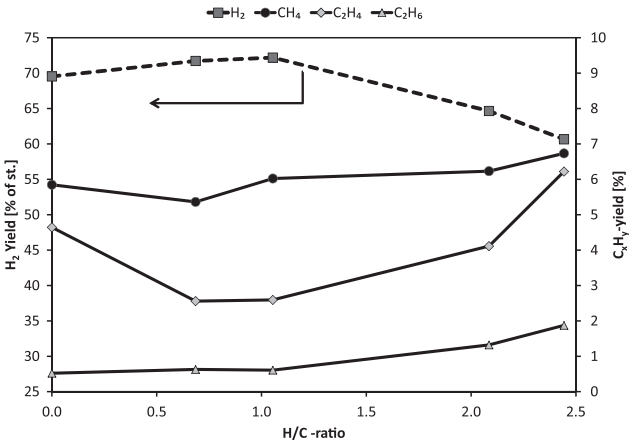

Fig. 7 – Yield of hydrogen, methane, and ethene as function of H/C-ratio over Ni/$MgAl_2O_4$. Full lines are hydrocarbon yields and dashed lines are hydrogen yield. Experimental conditions: S/C: 5.9–6.0; Temp.: 586–592 °C; m_{Cat} = 0.50 g, Ni loading: 8.2 wt%, F_T = 1600 N mL/min, y_{Eth} = 3.0–3.3 vol%, y_{H_2O} = 36.0–37.2 vol%, y_{H_2} = 0–7.4 vol%, N_2 as balance.

Hydrogen addition

Hydrogen addition to the feed was tested during SR of ethanol over a Ni/$MgAl_2O_4$ catalyst at 600 °C, S/C-ratio of roughly 6, and H_2/EtOH-ratio (H/C-ratio) between 0 and 2.5 (on molar basis). The conversion and carbon deposition as function of H/C-ratio can be seen in Fig. 6. The conversion increased from 73% at H/C = 0–81% at H/C = 1.1 and then decreased to 62% at H/C = 2.4. The decrease in conversion at H/C ≥1.1 is probably due to a shift in the WGS, Reaction (3), leading to fewer O- or OH-species on the catalyst surface to oxidize the carbon intermediates. This is discussed further in the Supplementary Data, where the surface reactions in WGS and SR of ethanol also are presented.

The carbon deposition as function of H/C-ratio can be seen in Fig. 6. There was a slight decrease in carbon deposition with increasing H/C-ratio. The decrease in carbon deposition might be due to increasing hydrogenation of C or CH_x-species or due to competitive adsorption between H_2 and ethanol derivatives leading to lower amounts of C on the surface.

The yield of H_2, CH_4, C_2H_4, and C_2H_6 as function of H/C-ratio is shown in Fig. 7. The yield of H_2 was not influenced at H/C-ratios between 0 and 1.1, but decreased at H/C-ratios higher than 1.1. This is expected as a higher concentration of H_2 will shift the WGS toward CO and H_2O (see Reaction (3)). The CO_2/CO-ratio decreased from 4.1 at H/C = 0 to 2.5 at H/C = 2.4 showing that the WGS indeed shifted to the left.

The yield of methane increased from 5.9% at H/C = 0 to 6.7% at H/C = 2.4, which was expected as an increase in the concentration of H_2 will shift the methanation reaction toward CH_4.

The MAR for WGS and methanation as function of H/C-ratio can be seen in Fig. S7 in the Supplementary Data. The MAR for methanation increased with H/C-ratio indicating that the equilibrium was approached with increasing H/C-ratio. The MAR for WGS decreased with increasing H/C-ratio, showing that the WGS moved further away from equilibrium with increasing H/C-ratio. The coverage of catalysts with H-species with increasing H/C-ratio could account for the decrease in the WGS activity.

The yield of ethene was 4.9% at H/C = 0 then decreased to a minimum of 2.6% at H/C = 1.1 and increased to 6.2 at H/C = 2.4. The decrease in the yield of ethene at H/C-ratios between 0 and 1.1 was probably due to increased rate of SR reactions as the conversion of ethanol also increased at H/C-ratios between 0 and 1.1. The increase in yield of ethene at H/C above 1.1 indicate a lower conversion of ethene, which could be due to a high coverage of hydrogen species on surface of the catalysts, H*, which limits the adsorption and conversion of ethene.

The yield of ethane increased from 0.52% at H/C = 0–1.9% at H/C = 2.4. This shows that the hydrogenation of ethene to ethane increased with increasing H/C-ratio as expected.

The principle of equilibrated and actual gas did not show potential for carbon formation, again indicating ethene as the primary source of carbon deposition.

The reaction network for SR of ethanol and how the result presented in this study compares with the literature is discussed in the Supplementary Data.

Stability tests

Oxidative SR and SR at a high S/C ratio both seemed interesting as they showed low carbon deposition and stable performance for 4 h during SR of ethanol at 600 °C. Therefore it was chosen to conduct SR of ethanol at these reaction conditions for 24 h to get a deeper understanding of the stability and rate of carbon deposition. The conversion and yield of hydrocarbons as function of time on stream for SR of ethanol at S/C-ratio of 6, 8, and at S/C = 6 and O/C = 0.8 can be seen in

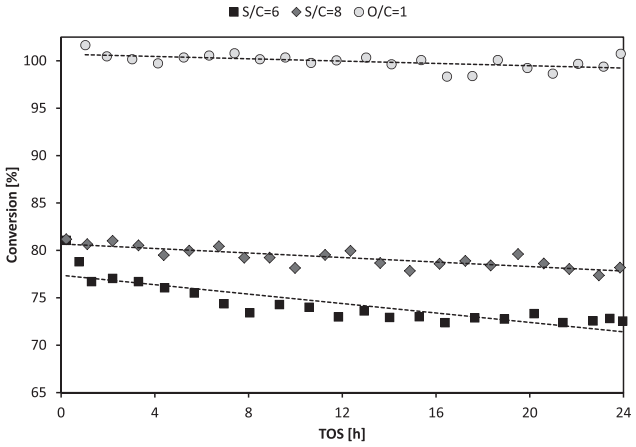

Fig. 8 – Conversion as function of time over Ni/$MgAl_2O_4$ OSR at O/C = 1 and S/C = 6, SR at S/C = 8, and SR at S/C = 6. Experimental conditions: Temp.: 590–606 °C, m_{Cat} = 0.50 g, Ni loading: 8.2 wt%, F_T = 1600 N mL/min, y_{Eth} = 3.2 %, y_{H_2O} = 40.1–51.5 vol%, y_{O_2} = 0–2.5 vol%, N as balance. Hydrocarbons are CH_4 and C_2H_4.

Figs. 8 and 9, respectively. The yield of hydrocarbons is the combined yield of CH_4 and C_2H_4. The conversion remained stable around 100% during the entire experiment for SR with oxygen present, while the two conditions without O_2 present showed deactivation. It was most pronounced for SR at S/C = 6, where the conversion decreased from 80% to 72% over 24 h, while the conversion at S/C = 8 decreased from 81% to 78%.

The total yield of hydrocarbons under OSR was stable around 3.5–4%, however an increase in the yield of ethene with time on stream from 0.2% after 1 h to 0.7% after 24 h was observed. The total yield of hydrocarbons was stable around 7% at S/C = 8 and the yield of ethene increased from 1.9% to

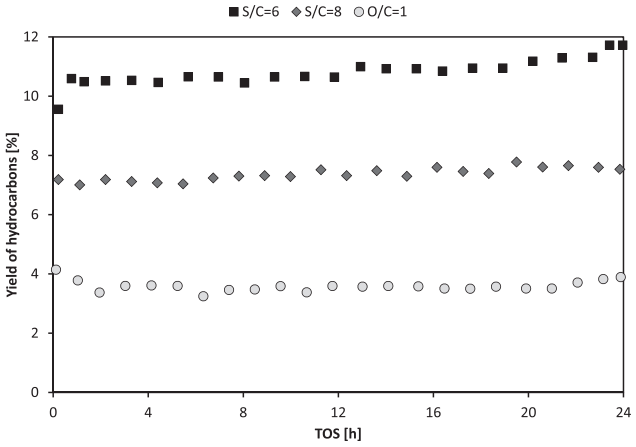

Fig. 9 – Yield of hydrocarbons as function of time over Ni/$MgAl_2O_4$ at OSR at O/C = 1 and S/C = 6, SR at S/C = 8, and SR at S/C = 6. Experimental conditions: Temp.: 590–606 °C, m_{Cat} = 0.50 g, Ni loading: 8.2 wt%, F_T = 1600 N mL/min, y_{Eth} = 3.2%, y_{H_2O} = 40.1–51.5 vol%, y_{O_2} = 0–2.5 vol%, N_2 as balance. Hydrocarbons are CH_4 and C_2H_4.

Table 5 – Comparison of conversion, yield of ethene, methane, and hydrogen in oxidative SR at S/C of 6 and O/C of 0.7 after 1 and 24 h on stream at different space velocities. Y: yield. Experimental conditions: Temp.: 606–608 °C, m_{Cat} = 0.27 or 0.50 g, Ni loading: 8.2 wt%, F_T = 1600 N mL/min, y_{Eth} = 3.2–3.8%, y_{H_2O} = 38.7–38.9 vol%, y_{O_2} = 2.5–2.8 vol%, N_2 as balance.

WHSV [h^{-1}]	Conversion		Y_{H_2}		Y_{CH_4}		$Y_{C_2H_4}$	
	1 h	24 h	1 h	24 h	1 h	24 h	1 h	24 h
12.6	100	100	56	54	3.4	3.1	0.2	0.7
28.3	99	97	50	48	6.3	6.8	2.7	3.2

3.5% during the experiment. The yield of hydrocarbons for SR of ethanol at S/C = 6 increased from 10% to 12% over 24 h, due to an increase in the yield of ethene from 4.4% to 7.7% and a decrease in the yield of CH_4. Both conversion and yield of hydrocarbons as functions of time showed that more stable behavior was achieved by adding either additional water or O_2.

The conversion with oxygen present was 100% for the entire 24 h experiment and therefore the experiment was repeated with a lower mass of catalyst to attempt to obtain less than full conversion. A comparison of conversion, yield of ethene, methane, and hydrogen both initially and after 24 h at the two different space velocities (SV) can be seen in Table 5. As expected the conversion decreased while the yield of hydrocarbons increased with increasing SV. A slight deactivation at the higher SV over 24 h could be observed as conversion and yield of H_2 decreased with time, while the yield of both methane and ethene increased with time.

The carbon deposition after 4 h and 24 h during SR at S/C = 6, SR at S/C = 6 with O/C = 0.8, and SR at S/C = 8 can be seen in Table 6. In general, the rate of carbon deposition decreased with time for the three cases. At S/C = 6 the total amount of carbon on the catalyst decreased from 4 to 24 h on stream, which could indicate that the carbon deposition had reached a steady state and would remain at this level. However, an additional experiment with 100 h on stream had a total carbon deposition of 106 mg compared 54 mg after 24 h, so the carbon deposition did still increase with time on stream. The conversion also decreased with time on stream

Table 6 – Carbon deposition after 4 and 24 h for SR at S/C = 6, SR at S/C = 6 with O/C = 1, and SR at S/C = 8. Experimental conditions: Temp.: 576 °C, m_{Cat} = 0.27 or 0.50 g, Ni loading: 8.2 wt%, F_T = 1600 NL/min, WHSV = 12.9 or 28.3 h^{-1}, y_{Eth} = 3.3%, y_{H_2O} = 39.5–51.5 vol%, y_{O_2} = 0–3.2 vol%, N_2 as balance.

Type	TOS	Carbon deposition		
		[mmole C/mole C_{Feed}]	[mg C/g_{Cat} h]	[mg]
SR at S/C = 6	4	4.4	28.0	56
SR at S/C = 6	24	0.7	4.5	54
SR at S/C = 8	4	1.8	11.4	23
SR at S/C = 8	24	0.7	4.7	56
SR at O/C = 0.8	4	0.03	0.2	0.4
SR at O/C = 0.8	24	0.018	0.12	1.4
SR at O/C = 0.7 and WHSV = 28.3 h^{-1}	24	0.011	0.16	1.0

Table 7 – BET surface area and Ni particle size for Ni/$MgAl_2O_4$ before and after operation at S/C = 6, S/C = 8, and O/C = 1 and 600 °C for 24 h. XRD analysis used to determine the particle size using the NiO reflection peak at $2\theta = 62.8°$.

	Surface area [m^2/g]	NiO particle size [nm]
Fresh	98	4
SR at S/C = 6	84	6
SR at S/C = 8	79	7
SR at O/C = 0.8	69	9

during the entire 100 h. The conversion, yield of hydrocarbons, and yield of H_2 as function of time on stream for the 100 h experiment can be seen in Fig. S8 in the Supplementary Data. The apparent stable level of carbon deposition between 4 and 24 h and increase in carbon deposition after 100 h could indicate that two mechanisms of carbon deposition occurred; An initial laydown of carbon and then after, an induction period, a second laydown of carbon occurs. The initial carbon deposition could be on very active step sites, while the second type of carbon could be due to whisker formation [34]. This type of carbon would form when the Ni-particles have sintered to a minimum size at which whisker formation is possible [32,34]. An induction period with no carbon deposition followed by a period with a constant rate of carbon deposition has also been reported in SR of hydrocarbons [29,31,54].

Oxidative steam reforming seems to be most promising as the lowest carbon deposition and highest conversion can be achieved with this feed. Furthermore, at the more severe conditions (higher SV), where the ethene fraction in the offgas was higher, the carbon deposition was still low.

The surface area and NiO particle size for fresh Ni/$MgAl_2O_4$ and spent Ni/$MgAl_2O_4$ after 24 h on stream at S/C = 6, S/C = 8, and O/C = 0.8 and after oxidation of the carbon deposits can be seen in Table 7. The NiO particle size increased and surface area decreased with time-on-stream indicating that sintering of the Ni particles and support material occurred at all of the conditions investigated. The sintering was most pronounced with oxygen present and could account for the deactivation seen in OSR despite the low carbon deposition. No Ni peaks were observed in the XRD-spectra so the change in the particle size of NiO can be related to the change in particle size of Ni.

Carbon deposition was not completely inhibited during SR at O/C below 1 and therefore an additional long term stability test was conducted at an even higher O/C-ratio. The yield of hydrocarbons and H_2 as well as conversion and CO_2/CO-ratio as function time on stream during SR at O/C = 1.1 can be seen in Fig. 10. The CO_2/CO-ratio decreased while the yield of methane and ethene both increased during the first 30 h on stream and hereafter remained stable for the next 60 h. The increase in yield of hydrocarbons and drop in yield of H_2 after 24 h on stream was due to a short malfunction of the feeding system, which the caused the feed of H_2O and ethanol to stop for a short period of time (5–10 s). Therefore O_2 in N_2 could reach the catalyst and cause a slight oxidation of the catalyst.

The total carbon deposition after 90 h on stream was 0.1 mg, corresponding to $0.2 \cdot 10^{-3}$ mmole C/mole C_{Feed}. The

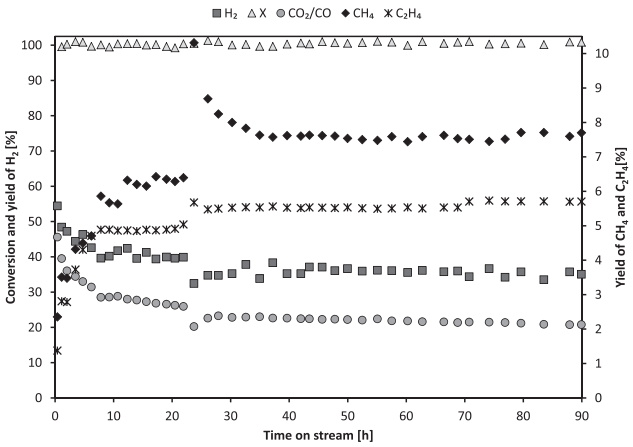

Fig. 10 – Conversion, CO_2/CO-ratio, yield of hydrocarbons, and yield of H_2 as function of time at O/C = 1.1 and S/C = 6 over Ni/$MgAl_2O_4$. Experimental conditions: Temp.: 617 °C, m_{Cat} = 0.36 g, Ni loading: 8.2 wt%, F_T = 1600 N mL/min, y_{Eth} = 3.6%, y_{H_2O} = 37.8 vol%, y_{O_2} = 4 vol%, N_2 as balance.

stable behavior with time-on-stream and low amount of carbon on catalyst shows that oxidative SR of ethanol at O/C-ratio above 1 are needed for stable operation with very low rate of carbon deposition (7 μg C/g_{Cat} h) over Ni/$MgAl_2O_4$. Due to the high content of O_2 in the feed it might be possible to lower the S/C-ratio as the main purpose of the steam might be to shift the gas and not to keep the catalysts free of coke.

The penalty of the more stable performance of the catalysts is a loss in H_2 production of respectively 1 or 2 mole of H_2 pr. mole ethanol converted at O/C = 0.8 and at O/C = 1.1 compared with SR at S/C = 6 without O_2 addition. As mentioned above additional hydrogen may be obtained by fully converting the hydrocarbons and shifting the gas at 300 °C, by which the remaining CO is converted to CO_2 and H_2. In this way a total hydrogen yield of 59% or 3.6 moles of H_2 pr. mole of ethanol may optimally be obtained.

That oxidative SR of ethanol is required for stable operation was also concluded in the work of Salge et al. [42] and others [35,43,51,55] using noble metal catalysts. The present results indicate that the use of noble metal based catalysts may be avoided, since there is no obvious advantage relative to the presently tested Ni-based catalyst.

Conclusions

In this work the influence of feed gas composition in terms of O_2, H_2 and H_2O concentrations on SR of ethanol over Ni-based catalysts has been investigated at 600 °C. Most experiments were made using a Ni/$MgAl_2O_4$ catalyst but also Ni/CeO_2 and Ni/$Ce_{0.6}Zr_{0.4}O_2$ were investigated. Increasing the S/C-ratio from the stoichiometric value of 1.5 to 8.2 improved the performance of the catalyst significantly as the conversion of ethanol and yield of H_2 increased while the yield of hydrocarbons and carbon deposition decreased. The conversion was 80%, the yield of H_2 was 73%, and the rate of carbon deposition was 1.8 mmole C/mole C_{Feed} or 11.4 mg C/g_{Cat} h in a

4 h experiment at S/C-ratio of 8.2. The decrease in carbon deposition with increasing S/C-ratio was mainly ascribed to a faster conversion of ethene, which is a main intermediate species in the conversion of ethanol, and a severe precursor to carbon formation.

The addition of O_2 was particularly beneficial as conversion of ethanol increased while the yield of hydrocarbons and carbon deposition decreased with increasing O/C-ratio. Oxygen addition at an O/C-ratio of 0.8–1.0 decreased the carbon deposition to less than 0.02 mmole C/mole C_{Feed} or 0.2 mg C/g_{Cat} h over both Ni/$MgAl_2O_4$ and Ni/$Ce_{0.6}Zr_{0.4}O_2$. The penalty of adding oxygen was a loss in the yield of hydrogen from 70% to 50% when increasing the O/C-ratio from 0 to 0.8–1.0. The decrease in carbon deposition was probably due to oxidation of carbon, while the lower yield of H_2 was due to oxidation of H_2, CO and hydrocarbons to CO_2 and H_2O. The beneficial effects of adding O_2 to the feed over Ni/$MgAl_2O_4$ catalysts, decreased carbon deposition and increased conversion, was also found on Ni/CeO_2 and Ni/$Ce_{0.6}Zr_{0.4}O_2$ catalysts.

Addition of H_2 to the feed did not improve the SR of ethanol significantly with respect to conversion, carbon deposition, or yield of hydrocarbons. High amounts of H_2 in the feed led to lower conversion of ethanol, probably due to a high coverage of hydrogen preventing ethanol to react or a decrease in surface O-species on the catalysts.

A 90 h-test at 600 °C and O/C = 1.1 showed that stable operation and high conversion with very low rate of carbon deposition of 7 μg C/g_{Cat} h could be achieved over Ni/$MgAl_2O_4$. The results, in general, showed that oxidative SR of ethanol is the most promising method for enhancing the performance of Ni-based catalysts in SR of ethanol.

Acknowledgments

This work is part of the CHEC (Combustion and Harmful Emission Control) Research Center, EGSSE (European Graduate School of Sustainable Energy), and CASE (Catalysis for Sustainable Energy). The work is financed by the Technical University of Denmark and the Danish Ministry for Science, Technology and Development under the CASE initiative.

Appendix A. Supplementary data

Supplementary data related to this article can be found at http://dx.doi.org/10.1016/j.ijhydene.2014.03.107.

REFERENCES

[1] Raffelt K, Henrich E, Koegel A, Stahl R, Steinhardt J, Weirich F. The BTL2 process of biomass utilization entrained-flow gasification of pyrolyzed biomass slurries. Appl Biochem Biotechnol 2006;129:153–64.
[2] Venderbosch RH, Prins W. Fast pyrolysis technology development. Biofuel Bioprod Bioref 2010;4:178–208.
[3] Mullen CA, Boateng AA, Hicks KB, Goldberg NM, Moreau RA. Analysis and comparison of bio-oil produced by fast pyrolysis from three barley biomass/byproduct streams. Energy Fuels 2010;24:699–706.
[4] Oasmaa A, Solantausta Y, Arpiainen V, Kuoppala E, Sipilä K. Fast pyrolysis bio-oils from wood and agricultural residues. Energy Fuels 2010;24:1380–8.
[5] Trinh TN, Jensen PA, Dam-Johansen K, Knudsen NO, Sørensen HR, Hvilsted S. Comparison of lignin, macroalgae, wood, and straw fast pyrolysis. Energy Fuels 2013;27:1399–409.
[6] Oasmaa A, Meier D. Norms and standards for fast pyrolysis liquids 1. Round robin test. J Anal Appl Pyrolysis 2005;73:323–34.
[7] Demirbas A. Competitive liquid biofuels from biomass. Appl Energy 2011;88:17–28.
[8] Qi Z, Jie C, Tiejun W, Ying X. Review of biomass pyrolysis oil properties and upgrading research. Energy Conv Manage 2007;48:87–92.
[9] Trane R, Jensen AD, Dahl S. Catalytic steam reforming of bio-oil. Int J Hydrogen Energy 2012;37:6447–72.
[10] Mortensen PM, Grunwaldt JD, Jensen PA, Knudsen KG, Jensen AD. A review of catalytic upgrading of bio-oil to engine fuel. Appl Catal A Gen 2011;407:1–19.
[11] Huber GW, Iborra S, Corma A. Synthesis of transportation fuels from biomass: chemistry, catalysts, and engineering. Chem Rev 2006;106:4044–98.
[12] Wang D, Czernik S, Montane D, Mann M, Chornet E. Biomass to hydrogen via fast pyrolysis and catalytic steam reforming of the pyrolysis oil or its fractions. Ind Eng Chem Res 1997;36:1507–18.
[13] Rioche R, Kulkarni S, Meunier FC, Breen JP, Burch R. Steam reforming of model compounds and fast pyrolysis bio-oil on supported noble metal catalysts. Appl Catal B Environ 2005;61:130–9.
[14] Basagiannis AC, Verykios XE. Steam reforming of the aqueous fraction of bio-oil over structured Ru/MgO/Al_2O_3 catalysts. Catal Today 2007;127:256–64.
[15] Czernik S, French R, Feik C, Chornet E. Hydrogen by catalytic steam reforming of liquid byproducts from biomass thermoconversion processes. Ind Eng Chem Res 2002;41:4209–15.
[16] Hu X, Lu G. Investigation of the steam reforming of a series of model compounds derived from bio-oil for hydrogen production. Appl Catal B Environ 2009;88:376–85.
[17] Hu X, Lu G. Bio-oil steam reforming, partial oxidation or oxidative steam reforming coupled with bio-oil dry reforming to eliminate CO_2 emission. Int J Hydrogen Energy 2010;35:7169–76.
[18] Cavallaro S, Chiodo V, Freni S, Mondello N, Frusteri F. Performance of Rh/Al_2O_3 catalyst in the steam reforming of ethanol: H_2 production for MCFC. Appl Catal A Gen 2003;249:119–28.
[19] Rass-Hansen J, Christensen CH, Sehested J, Helveg S, Rostrup-Nielsen JR, Dahl S. Renewable hydrogen: carbon formation on Ni and Ru catalysts during ethanol steam-reforming. Green Chem 2007;9:1016–21.
[20] Galetti AE, Gomez MF, Arrúa LA, Abello MC. Ni catalysts supported on modified $ZnAl_2O_4$ for ethanol steam reforming. Appl Catal A Gen 2010;380:40–7.
[21] Ni M, Leung D, Leung M. A review on reforming bio-ethanol for hydrogen production. Int J Hydrogen Energy 2007;32:3238–47.
[22] de Ávila CN, Hori CE, de Assis AJ. Thermodynamic assessment of hydrogen production and cobalt oxidation susceptibility under ethanol reforming conditions. Energy 2011;36:4385–95.
[23] Haryanto A, Fernando S, Murali N, Adhikari S. Current status of hydrogen production techniques by steam reforming of ethanol: a review. Energy Fuels 2005;19:2098–106.

[24] Fatsikostas AN, Verykios XE. Reaction network of steam reforming of ethanol over Ni-based catalysts. J Catal 2004;225:439–52.
[25] Benito M, Sanz JL, Isabel R, Padilla R, Arjona R, Daza L. Bio-ethanol steam reforming: insights on the mechanism for hydrogen production. J Power Sources 2005;151:11–7.
[26] Subramani V, Song C. Advances in catalysis and processes for hydrogen production from ethanol reforming. Cat 2007;20:65–106.
[27] Sanchez-Sanchez MC, Navarro RM, Fierro JLG. Ethanol steam reforming over Ni/M_xO_y-Al_2O_3 (M = Ce, La, Zr and Mg) catalysts: influence of support on the hydrogen production. Int J Hydrogen Energy 2007;32:1462–71.
[28] Trane-Restrup R, Resasco DE, Jensen AD. Steam reforming of light oxygenates. Catal Sci Technol 2013;3:3292–302.
[29] Rostrup-Nielsen JR. Coking of nickel catalysts for steam reforming of hydrocarbons. J Catal 1974;33:184–201.
[30] Rostrup-Nielsen JR. Steam reforming catalysts. Teknisk Forlag; 1975.
[31] Rostrup-Nielsen JR. Hydrogen via steam reforming of naphtha. Chem Eng Prog 1977;73:87–92.
[32] Rostrup-Nielsen JR, Christiansen LJ. Concepts in syngas manufacture. Imperial College Press; 2011.
[33] Rostrup-Nielsen JR, Sehested J, Nørskov JK. Hydrogen and synthesis gas by steam- and CO_2 reforming. Adv Catal 2002;47:65–139.
[34] Aasberg-Petersen K, Dybkjaer I, Ovesen CV, Skjøth NC, Sehested J, Thomsen SG. Natural gas to synthesis gas – catalysts and catalytic processes. J Nat Gas Sci Eng 2011;3:423–59.
[35] Deluga GA, Salge JR, Schmidt LD, Verykios XE. Renewable hydrogen from ethanol by autothermal reforming. Science 2004;303:993–7.
[36] Vagia EC, Lemonidou AA. Thermodynamic analysis of hydrogen production via autothermal steam reforming of selected components of aqueous bio-oil fraction. Int J Hydrogen Energy 2008;33:2489–500.
[37] Cavallaro S, Chiodo V, Vita A, Freni S. Hydrogen production by auto-thermal reforming of ethanol on Rh/Al_2O_3 catalyst. J Power Sources 2003;123:10–6.
[38] Platon A, Roh HS, King DL, Wang Y. Deactivation studies of $Rh/Ce_{0.8}Zr_{0.2}O_2$ catalysts in low temperature ethanol steam reforming. Top Catal 2007;46:374–9.
[39] Medrano JA, Oliva M, Ruiz J, Garcìa L, Arauzo J. Catalytic steam reforming of acetic acid in a fluidized bed reactor with oxygen addition. Int J Hydrogen Energy 2008;33:4387–96.
[40] Schmidt L, French R, Czernik S, Josephson T, Rennard D. Production of synthesis gas by partial oxidation and steam reforming of biomass pyrolysis oils. Int J Hydrogen Energy 2010;35:4048–59.
[41] de Lima SM, da Silva AM, da Costa LOO, Assaf JM, Mattos LV, Noronha FB, et al. Hydrogen production through oxidative steam reforming of ethanol over Ni-based catalysts derived from $La_{1-x}Ce_xNiO_3$ perovskite-type oxides. Appl Catal B Environ 2012;121–122:1–9.
[42] Salge JR, Deluga GA, Schmidt LD. Catalytic partial oxidation of ethanol over noble metal catalysts. J Catal 2005;235:69–78.
[43] Peela NR, Kunzru D. Oxidative steam reforming of ethanol over Rh based catalysts in a micro-channel reactor. Int J Hydrogen Energy 2011;36:3384–96.
[44] Laosiripojana N, Assabumrungrat S, Charojrochkul S. Steam reforming of ethanol with co-fed oxygen and hydrogen over Ni on high surface area ceria support. Appl Catal A Gen 2007;327:180–8.
[45] Jacobs G, Keogh RA, Davis BH. Steam reforming of ethanol over Pt/ceria with co-fed hydrogen. J Catal 2007;245:326–37.
[46] Trane-Restrup R, Dahl S, Jensen AD. Steam reforming of ethanol: effects of support and additives on Ni-based catalysts. Int J Hydrogen Energy 2013;38:15105–18.
[47] Moulijn JA, van Diepen AE, Kapteijn F. Activity loss. Handbook of heterogeneous catalysis. Wiley-VCH; 2010. pp. 1–17.
[48] Logsdon JE. Ethanol. Kirk-Othmer encyclopedia of chemical technology. Wiley; 2004.
[49] Gallezot P, Bergeret G. Characterization of solid catalysts. Handbook of heterogeneous catalysis. Wiley-VCH; 2010. pp. 738–65.
[50] Fogler HS. Elements of chemical reaction engineering. 4th ed. Prentice Hall; 2006.
[51] Cai W, Wang F, Daniel C, van Veen AC, Schuurman Y, Mirodatos C, et al. Oxidative steam reforming of ethanol over Ir/CeO_2 catalysts: a structure sensitivity analysis. J Catal 2012;286:137–52.
[52] Laosiripojana N, Sangtongkitcharoen W, Assabumrungrat S. Catalytic steam reforming of ethane and propane over CeO_2-doped Ni/Al_2O_3 at SOFC temperature: improvement of resistance toward carbon formation by the redox property of doping CeO_2. Fuel 2006;85:323–32.
[53] Barattini L, Ramis G, Resini C, Busca G, Sisani M, Constantino U. Reaction path of ethanol and acetic acid steam reforming over Ni-Zn-Al catalysts. Flow reactor studies. Chem Eng J 2009;153:43–9.
[54] Rostrup-Nielsen JR. Steam reforming. Handbook of heterogeneous catalysis. Wiley-VCH; 2010. pp. 2882–905.
[55] Hung CC, Chen SL, Liao YK, Chen CH, Wang JH. Oxidative steam reforming of ethanol for hydrogen production on M/Al_2O_3. Int J Hydrogen Energy 2012;37:4955–66.